Published in final edited form as:
Hepatology. 2014 May ; 59(5): 1984–1997. doi:10.1002/hep.26976.

Hepatocyte specific HMGB1 deletion worsens the injury in liver ischemia/reperfusion: A role for intracellular HMGB1 in cellular protection

Hai Huang[#1], **Gary W. Nace**[#1], **Kerry-Ann McDonald**[1], **Sheng Tai**[1], **John R. Klune**[1], **Brian R. Rosborough**[1], **Qing Ding**[1], **Patricia Loughran**[1,2], **Xiaorong Zhu**[3], **Donna Beer-Stolz**[2], **Eugene B. Chang**[3], **Timothy Billiar**[1], and **Allan Tsung**[1]

[1]Department Of Surgery, University of Pittsburgh Medical Center, Pittsburgh, PA.

[2]Center for Biologic Imaging, Department of Cell Biology, University of Pittsburgh Medical Center, Pittsburgh, PA.

[3]Department of Medicine, University of Chicago, Chicago, IL

[#] These authors contributed equally to this work.

Abstract

High mobility group box-1 (HMGB1) is an abundant chromatin associated nuclear protein and released into the extracellular milieu during liver ischemia/reperfusion (I/R), signaling the activation of pro-inflammatory cascades. Since the intracellular function of HMGB1 during the sterile inflammation of I/R is currently unknown, we sought to determine the role of intracellular HMGB1 in hepatocytes following liver I/R. When hepatocyte specific HMGB1 knockout (HMGB1-HC-KO) and control mice were subjected to a non-lethal warm liver I/R, it was found that HMGB1-HC-KO mice had significantly greater hepatocellular injury after I/R compared to control mice. Additionally, there was significantly greater DNA damage and decreased chromatin accessibility to repair with lack of HMGB1. Furthermore, lack of hepatocyte HMGB1 led to excessive poly (ADP-ribose) polymerase-1 (PARP-1) activation, exhausting NAD^+ and ATP stores, exacerbating mitochondrial instability and damage, and consequently leading to increased cell death. We found that this was also associated with significantly more oxidative stress in HMGB1-HC-KO mice compared to control. Increased nuclear instability led to a resultant increase in the release of histones with subsequently more inflammatory cytokine production and organ damage through the activation of TLR9.

Conclusion—Therefore, the lack of HMGB1 within hepatocytes leads to the increased susceptibility to cellular death after oxidative stress conditions.

Contact Information: Name: Allan Tsung tsunga@upmc.edu Telephone number: 412-692-2001 Fax number: 412-692-2002 Postal address: 3459 Fifth Avenue UPMC Montefiore, 7 South Pittsburgh, PA 15213-2582.
Hai Huang: huangh2@upmc.edu; Gary W. Nace: nacegw@upmc.edu; Kerry-Ann McDonald: stewarkc@upmc.edu; Sheng Tai: taisheng1973@gmail.com; John R. Klune: klunejr@upmc.edu; Brian R. Rosborough: rosborough.brian@medstudent.pitt.edu; Qing Ding: dingq@upmc.edu; Patricia Loughran: loughranp@upmc.edu; Xiaorong Zhu: xzhu1@uchicago.edu; Donna Beer-Stolz: dstolz@pitt.edu; Eugene B. Chang: echang@medicine.bsd.uchicago.edu; Timothy Billiar: billiartr@upmc.edu; Allan Tsung: tsunga@upmc.edu

Conflict of Interest Statement: The authors have no conflicts of interest to disclose.

Keywords

Sterile inflammation; ischemia/reperfusion injury; danger associated molecular pattern molecules; hepatocytes; HMGB1

INTRODUCTION

Ischemia-reperfusion (I/R) injury is a process whereby an initial hypoxic insult and subsequent return of blood flow leads to the propagation of an innate immune response and ensuing organ injury. Although the liver may initially exhibit direct cellular damage as the result of the ischemic insult, reperfusion further propagates dysfunction and damage resulting from the activation of inflammatory pathways (1). Central to the propagation of this sterile inflammatory response is the recognition of damage associated molecular pattern molecules (DAMPs) by pattern recognition receptors (PRRs). Several DAMPs, including High mobility group box-1 (HMGB1), histones (2), and DNA as well as the PRRs, TLR4 and TLR9, have been shown to be involved in the damage and inflammation induced by warm liver I/R. We have shown previously that TLR4 signaling is crucial for the hepatic I/R response, and that this response is mediated by HMGB1 (3, 4).

HMGB1 is an evolutionarily conserved protein present in the nucleus of almost all eukaryotic cells (5). The function of HMGB1 is diverse and compartment specific. Outside the cell, HMGB1 exhibits a variety of activities that are dependent on the redox status of the protein. When mobilized to the cytoplasm, HMGB1 can regulate autophagic flux (6). Additionally, within the nucleus, HMGB1 facilitates gene transcription and the DNA repair response (7). HMGB1 has been identified as possibly playing a role in all 4 major DNA repair pathways: nucleotide excision repair (NER), mismatch repair, base excision repair (BER), and DNA double-strand break repair (8). Furthermore, we have previously shown that HMGB1 is rapidly mobilized to the cytoplasm and the extracellular space in hepatocytes following ischemia *in vivo* or hypoxia *in vitro* (9). The function of HMGB1 in specific cell types during the injury response has been difficult to fully elucidate secondary to the fact that mice lacking functional HMGB1 die shortly after birth. Therefore, in order to further investigate the role of HMGB1 within the hepatic I/R response we used novel transgenic cell-specific knockout (KO) mice, generated using Cre-*loxP* technology, in which hepatocytes are deficient in HMGB1. Knockout of HMGB1 specifically within hepatocytes is ideally suited to further investigate the role of HMGB1 in hepatic I/R since we have recently shown that not only do hepatocytes a play a key role in the inflammatory response associated with I/R, but also that hepatocytes are a major cell type responsible for TLR4 dependent HMGB1 release after I/R (10).

In this study we found that deletion of HMGB1 from hepatocytes resulted in greater liver injury following I/R. This is in striking contrast to the pro-inflammatory role of extracellular HMGB1, these studies reveal a dominant role for intracellular HMGB1 in stabilizing the nuclear response to oxidative stress.

MATERIAL AND METHODS

Animals

Male wild-type ($HMGB1^{loxP/loxP}$) mice, hepatocyte specific $HMGB1^{-/-}$ mice were bred at our facility and used at the age of 8-12 weeks. All mice developed were on a C57BL/6 genetic background. Animal protocols were approved by the Animal Care and Use Committee of the University of Pittsburgh and the experiments were performed in strict adherence to the NIH Guidelines for the Use of Laboratory Animals.

Generation of $HMGB1^{loxP/loxP}$ and hepatocyte specific $HMGB1^{-/-}$ mice

In brief, the $HMGB1^{loxP}$ allele was created by inserting *loxP* sites within intron 1 and intron 2, flanking exon 2 of HMGB1. Overview of this construct is shown (Supplemental Fig.1A). Mice homozygous for $HMGB1^{loxP}$ were generated by Ozgene (Bentley, WA). $HMGB1^{loxP/loxP}$ mice were interbred with stud males ($HMGB1^{loxP/-;\ Alb\text{-}cre}$) to generate the desired genotype. Mice homozygous for Cre recombinase linked to the albumin (*alb*) promoter are commercially available from Jackson. Transgenic male mice used for experiments were confirmed to be desired genotype via standard genotyping techniques. Control mice used in this study were $HMGB1^{loxP/loxP}$ mice without the introduction of Cre recombinase.

Confirmation and characterization of transgenic $HMGB1^{-/-}$ mice

Isolation and determination of HMGB1 mRNA expression was performed as previously described (10) using specific primers as follows: Forward 5′-CACAGCCATTGCAGTACATTGA-3′ and Reverse 5′-TGCTTGTCATCTGCTGCAGTGT-3′ for HMGB1, and β-actin primers as described previously (4). University of Pittsburgh Genomics and Proteomics Core Laboratories performed mRNA microarray expression analysis using Illumina bead-array platform with Mouse Refseq8 BeadChip. Un-stimulated hepatocytes were isolated from either KO or control mice, allowed to stabilized overnight in culture and mRNA was isolated using Qiagen RNeasy Mini Kit (Valencia, CA). Experiment was performed using 2 mice from each strain with duplicate samples of each and expression was normalized using the cubic spline method.

Liver ischemia/reperfusion

A nonlethal model of segmental (70%) hepatic warm ischemia and reperfusion was used previously described (11). Mice received the TLR9 antagonist (ODN2088; 100μg per mouse; Invivogen) or PARP-1 inhibitor (3-AB, 20mg/kg; PJ-34, 10mg/kg; Sigma-Aldrich), or respective control intraperitoneally 1h prior to ischemia. Sham animals underwent anesthesia, laparotomy, and exposure of the portal triad without hepatic ischemia.

Isolation, culture, and treatment of hepatocytes and non-parenchymal cells

Hepatocytes and NPCs were isolated, plated, and exposed to hypoxia as previously described (11). Supernatants from hypoxic hepatocytes were harvested after a 12h hypoxic period and were used as conditioned media in subsequent co-culture assays.

Liver damage assessment

Serum alanine aminotransferase (sALT) levels, serum Aspartate transaminase (sAST), and baseline serum chemistry values were measured using the DRI-CHEM 4000 Chemistry Analyzer System (HESKA). The extent of parenchymal necrosis in the ischemic lobes was evaluated using H&E stained histological sections at 40× magnification (12). The necrotic area was quantitatively assessed by using Image J (NIH). Results were presented as the mean of percentage of necrotic area (mm^2) with respect to the entire area of one capture (mm^2).

ELISA

Serum TNF-α and IL-6 levels in the mouse were detected by ELISA kit (R&D Systems). HMGB1 was quantified using ELISA kit (IBL International). Serum histone quantification was performed using Cell Death Kit (Roche).

Immunoblotting

Western blot assay was performed using whole cell lysates from either liver tissue or hepatocytes, or media as previously described (4). Membranes were incubated overnight using the following antibodies: HMGB1 (Abcam) and β-actin (Sigma); phospho-p38, p38, phospho-JNK, JNK, ERK, phospho-ERK, p65, phospho-p65, PARP-1, acetyl-histone H3, acetyl-histone H4, and phospho-histone H2A.X (Cell Signaling); PAR (BD bioscience).

Immunofluorescent staining

For immunofluorescence staining, liver sections were fixed, stained, and imaged using confocal microscopy as previously described (13). The level of lipid peroxidation was determined by measuring a major aldehyde product of lipid oxidation, 4-hydroxy-2-nonenal (4-HNE) Michael adducts, with HNE antibody (1:200; Calbiochem). Liver tissue or hepatocytes were incubated with the specific primary antibodies for HMGB1 (1:1000, Abcam), histone H3 (1:500; Abcam) as previously described (14).

Quantitation of confocal immunofluorescence

All images were quantitated for 4-HNE or histone H3 using MetaMorph™ software (Molecular Devices, Downingtown, PA) as previously described (15).

SYBR green qRT-PCR

Total RNA was extracted from the liver tissue or NPCs using the RNeasy Mini Kit (Qiagen). mRNA for TNF-α, IL-6, ICAM-1, MCP-1, CXCL-10, IL-1β, IL-12p35, INF-β and β-actin was quantified in triplicate by SYBR Green qRT-PCR. PCR reaction mixture was prepared using SYBR Green PCR Master Mix (Applied Biosystems) using described primers (11).

Detection of cellular ROS production

After hypoxia, hepatocytes were stained by using DCF-DA cellular ROS detection assay kit (Abcam) according to the manufacturer's instructions then read in a fluorescence

spectrophotometer (SpectraMAX Gemini XS; MDS Analytical Technologies) as described previously (3).

ATP, NAD^+, and LDH quantification

Quantification of NAD^+, ATP and LDH levels from hepatocytes after hypoxia was performed by using NAD/NADH assay kit, ATP assay kit and LDH assay kit (Abcam).

Transmission Electron Microscopy (TEM)

At the end of 6h reperfusion, liver tissue was harvested following perfusion with PBS then fixed and processed for TEM as described previously (16). After dehydration, thin sections (70nm) were stained with uranyl acetate and lead citrate for observation under a JEM 1011CX electron microscope (JEOL, Peabody, MA). Images were randomly selected from a pool of 18 fields from within 5 grid squares under each condition.

Flow cytometry analysis

Ischemic liver lobes were aseptically harvested from HMGB1-HC-KO and control mice after 1h of ischemia and 6h of reperfusion and prepared as a single cell suspension. Samples were prepared and analyzed with flow cytometry for innate immune cell populations using the following antibodies as described (17): neutrophils ($CD11b^+Ly6G^+$), inflammatory monocytes ($CD11b^+Ly6C^{hi}$), and NK cells ($NK1.1^+CD11C^+$). Antibodies were purchased from eBioscience: PE anti-NK1.1 PK136 and PE-Cy7 anti-CD11b M1/70, BD Bioscience: APC anti-CD11c HL3 and FITC anti-Ly6C AL-21, or Biolegend: FITC anti-I-Ab AF6-120.1, APC anti-CD11b M1/70, PE-Cy7 anti-Ly6G 1A8.

For measurement of mitochondria-associated ROS production, hepatocytes were stained with MitoSOX (Molecular Probes/Invitrogen) following the manufacture's protocol for FACS analysis. For measurement of mitochondrial polarization, TMRE-mitochondrial membrane potential assay kit (Abcam) was used according to the manufacturer's instructions. For measurement of damaged mitochondria, hepatocytes were stained with Mitotracker green and Mitotracker deep red for FACS analysis.

Data were acquired with a BD FACS LSR Fortessa flow cytometer (BD Biosciences) and analyzed with FlowJo analytical software (Treestar). Each experiment was repeated a minimum of three times.

Statistical analysis

Results are expressed as either standard error of the mean (SEM) or mean standard deviation (SD). Group comparisons were performed using ANOVA and Student's t-test. A $p<0.05$ was considered statistically significant.

RESULTS

Confirmation of HMGB1 knockout mice

To investigate the roles of HMGB1 in hepatocytes, we generated HMGB1-HC-KO mice using Cre-*loxP* technology. Both control and HMGB1-HC-KO mice were born healthy and

fertile, without any grossly apparent phenotypic differences or abnormalities in liver function tests (Supplemental Fig.1B). Additionally, baseline differences in mRNA expression in un-stimulated hepatocytes were determined using microarray analysis. Surprisingly, a paucity of significant differences was found in hepatocyte mRNA expression of HMGB1-HC-KO mice compared against control at baseline (Supplemental Fig.1C).

Verification of the specificity of the HMGB1 knockout in the HMGB1-HC-KO mice was demonstrated by isolating hepatocytes, and analyzing these cells for the presence of HMGB1 mRNA expression using RT-PCR with primers specific for exon 2 of HMGB1 (Fig.1A). HMGB1 was confirmed Western blot that present in both hepatocytes and NPCs of the control mice, whereas the HMGB1-HC-KO mice had HMGB1 expressed only in the NPCs (Fig.1B). Immunofluorescent staining in hepatocytes isolated from the HMGB1-HC-KO mice had undetectable HMGB1 compared with HMGB1 positive hepatocytes from the control mice (Fig.1C).

Serum HMGB1 release after hepatic I/R is dependent on hepatocyte HMGB1

HMGB1 is rapidly mobilized and released in the setting of hepatic I/R and when released into the extracellular space, acts as a DAMP (3, 4). Since hepatocytes are a major source of HMGB1 after hepatic I/R (10), we anticipated that there would be substantially less circulating HMGB1 after I/R in KO mice and indeed HMGB1-HC-KO mice had significantly lower serum and intrahepatic HMGB1 levels compared to control mice (Fig.1D and Supplemental Fig.2A). Consistent with our previous results (4), HMGB1 localized to the nucleus of hepatocytes in control sham-treated animals. After I/R, HMGB1-positive staining was observed in the cytoplasm of hepatocytes. However, no HMGB1 positive hepatocytes were found in sham or I/R treated-HMGB1-HC-KO mice, again confirming that these mice do not express HMGB1 even after the stress of I/R (Fig.1E).

Genetic deletion of HMGB1 in hepatocytes exacerbates hepatic I/R injury

To determine the impact of hepatocyte HMGB1 deletion on the injury and inflammatory response induced by I/R, HMGB1-HC-KO mice were subjected to hepatic I/R. In the HMGB1-HC-KO mice, the sALT levels were significantly greater than control mice (Fig. 2A). The degree of liver damage on histologic analysis was concordant with the sALT results (Fig.2B and Supplemental Fig.2B). Additionally, serum levels of TNF-α and IL-6 were significantly higher in the HMGB1-HC-KO mice compared to the control mice (Fig. 2C). These results demonstrate that lack of HMGB1 in hepatocytes results in exacerbation of I/R injury and an exaggerated inflammatory response, a surprising finding given the defined role of HMGB1 as a pro-inflammatory DAMP.

Deletion of HMGB1 from hepatocytes results in enhanced inflammatory signaling following I/R

To further investigate how the lack of HMGB1 in hepatocytes might mediate the inflammatory response to hepatic I/R injury, we examined the Mitogen-activated protein (MAP) kinases and NF-κB signaling pathways. After 1h of hepatic I/R, phosphorylation of c-Jun N-terminal kinase (JNK), p38, extracellular signal-regulated kinase (ERK) and NF-κB (p65 subunit) increased compared to sham treated-mice. When HMGB1-HC-KO mice were

subjected to I/R, there was a much greater increase in the phosphorylation of all three MAPKs and NF-κB compared to control mice (Fig.3A), suggesting these mice have an increased inflammatory response after I/R.

The role of hepatocyte HMGB1 in modulating the recruitment of innate immune cells in the liver following I/R was determined by flow cytometry. As expected, liver I/R injury in control mice led to significantly greater recruitment of neutrophils, inflammatory monocytes, and NK cells compared with sham control mice (Fig.3B and Supplemental Fig. 3). However, the ablation of HMGB1 in hepatocytes lead to even greater recruitment of innate immune cells after liver I/R compared to control. Additionally, the quantification of chemokine expression revealed that HMGB1-HC-KO mice have increased expression of chemokines after I/R (Supplemental Fig.4). This data demonstrates that the elimination of HMGB1 in hepatocytes up-regulates the innate immune response by increasing chemokine expression and subsequent influx of inflammatory cells in the ischemic lobes after liver I/R.

Loss of HMGB1 in hepatocytes leads to nuclear instability with increased DNA damage and histone release

Knowing that HMGB1 has an important role in DNA repair (8, 18), we next sought to determine whether lack of HMGB1 in hepatocytes leads to increased oxidative DNA damage following the oxidative stress of I/R. Histone acetylation has previously been shown to be a sensitive marker for chromatin accessibility, with acetylated histones allowing for DNA access to repair enzymes (19). Acetylation of both histone H3 and H4 was markedly increased in the liver I/R treated control mice compared with sham control (Fig.4A). However, the acetylation of histone H3 and H4 was significantly lower after liver I/R injury in HMGB1-HC-KO mice, suggesting that there is decreased accessibility of chromatin for repair without HMGB1. In addition, histone H2A.X has been shown to be phosphorylated in response to DNA damage, serving as a marker of DNA damage (19). We found that the loss of HMGB1 within hepatocytes resulted in higher level of H2A.X phosphorylation after liver I/R injury compared with control mice (Fig.4A).

Consequential to our findings of increased DNA damage after oxidative stress in the livers of HMGB1-HC-KO mice, we investigated whether HMGB1 deletion resulted in the enhanced release of nucleosome components, such as histones. Histones are released from damaged hepatocytes both *in vitro* after hypoxia and *in vivo* after liver I/R injury and function as DAMPs to propagate injury (14). Although serum histone levels increased in both HMGB1-HC-KO and control mice after liver I/R, the levels in HMGB1-HC-KO mice were significantly higher compared to control mice at 6h after I/R injury (Fig.4B). Additionally, using immunofluorescence it was seen that histone H3 translocation from nucleus to cytoplasm occurred in both HMGB1 KO and control hepatocytes after hypoxia, but significantly more histone-positive staining was observed in the cytoplasm of HMGB1 KO hepatocytes (Fig.4C). Concordant results were observed in the media of hepatocytes under hypoxia by using Western blot analysis (Fig.4D). Thus, we conclude that the loss of HMGB1 results in increased DNA damage and release of nucleosome components leading to greater injury following oxidative stress.

PARP-1 over-activation in cells lacking HMGB1 leads to mitochondria damage by exhausting NAD^+ and ATP stores

Our above results suggest that the lack of HMGB1 in hepatocytes leads to excessive nuclear damage after oxidative stress. Upon DNA damage, the nuclear enzyme poly (ADP-ribose) polymerase-1 (PARP-1) consumes NAD^+ to form branched polymers of ADP-ribose (PAR) on target proteins, which include histones and PARP-1 itself. Poly (ADP-ribosylation) facilitates DNA repair by preventing chromatid exchange and by loosening histone wrapping (20). However, PARP-1 over-activation leads to cell death, presumably through mechanisms linked to NAD^+ depletion (21). Therefore, we sought to determine whether HMGB1 deletion in hepatocytes undergoing oxidative stress would result in excessive activation of PARP-1. We found that both PAR formation and PAR-PARP-1 were increased in the livers of both HMGB1-HC-KO and control mice after I/R injury. However, PARP-1 activity in the livers of HMGB1-HC-KO mice was significantly higher than in control mice after I/R (Fig.5A), suggesting that lack of HMGB1 leads to increased activation of PARP-1.

We next sought to confirm that the differences in PARP-1 activation led to altered NAD^+ and ATP levels in hepatocytes under hypoxic oxidative stress. In fact there was a significantly greater reduction of NAD^+ and ATP levels as early as 1h during hypoxia in HMGB1 KO hepatocytes compared with control hepatocytes (Fig.5B and 5C). Exhaustion of NAD^+ and ATP stores by hyper-activation of PARP-1 has previously been shown to lead to mitochondrial mediated-cell death (22). Consequently, we next explored if this reduced energy preservation in HMGB1 KO hepatocytes would alter mitochondrial function under oxidative stress. We demonstrated that a significantly greater loss of mitochondrial membrane potential was found in HMGB1 KO hepatocytes compared with control hepatocytes after hypoxia (Fig.5D). Additionally, HMGB1 KO hepatocytes had a significantly higher percentage of damaged mitochondria when exposed to hypoxia (Fig. 5E). This increased mitochondrial damage was further demonstrated morphologically by TEM with differences in mitochondrial ultrastructure and different stages of mitochondrial breakdown; suggesting inadequate removal of damaged mitochondria in HMGB1 KO hepatocytes not seen in control cells (Fig.5F). These findings lead us to conclude that the increased cellular injury with oxidative stress seen with lack of HMGB1 may be secondary to mitochondrial damage and dysfunction.

Hepatocytes lacking HMGB1 exhibit increased ROS production and cell death after oxidative stress

Mitochondrial dysfunction can perpetuate the production of ROS during oxidative stress (23). So, we sought to discern whether the lack of HMGB1 in hepatocytes influenced ROS production during oxidative stress. Interestingly, we found that there were higher levels of mitochondrial ROS in hepatocytes lacking HMGB1 compared to control hepatocytes exposed to hypoxia (Fig.6A). Additionally, HMGB1 KO hepatocytes also displayed a significant increase in total cellular ROS production after stimulation with hypoxia (Fig.6B).

To examine if HMGB1-HC-KO mice exhibit more oxidative damage after liver I/R, we measured 4-HNE Michael adducts, a marker of oxidative stress (24). We found a marked increase in the formation of 4-HNE after hepatic I/R in control mice compared to sham

control mice (Fig.6C). However, the increase in 4-HNE seen in the liver of HMGB1-HC-KO mice subjected to I/R was much greater compared to the control I/R livers (Fig.6D). Altogether, these results suggest that loss of HMGB1 in hepatocytes results in more oxidative stress in the liver following I/R injury. Furthermore, greater cell death in HMGB1 KO hepatocytes was confirmed by measuring LDH release from hepatocytes in the culture supernatants after hypoxia exposure (Fig.6E).

Histone-mediated inflammation through TLR9 is enhanced in mice lacking hepatocyte HMGB1

We have recently shown that histone release after liver I/R is a major contributor to inflammation and organ damage through a TLR9-dependent mechanism (14). Our above findings demonstrate that loss of HMGB1 in hepatocytes may lead to nuclear instability with histone release. To determine if increased histone release contributed to the worsened liver injury after I/R in HMGB1-HC-KO mice, we used the supernatants from hypoxic hepatocytes to stimulate hepatic NPCs. TNF-α, IL-6 and IL-1β mRNA levels were significantly increased in NPCs after treatment with media from hypoxic HMGB1 KO hepatocytes compared to media from hypoxic control hepatocytes (Fig.7A and Supplemental Fig.5A). Interestingly, this effect was reduced by treatment with the TLR9 inhibitor (ODN2088) (Fig.7A). We also treated both HMGB1-HC-KO and control mice with a TLR9 inhibitor during liver I/R and found that the increased liver damage and cytokine production seen in mice lacking hepatocyte HMGB1 was significantly reduced (Fig.7B and Supplemental Fig.5B). Thus, these results suggest that the lack of HMGB1 may also increase hepatocellular injury by enhancing histone-dependent TLR9 activity.

Inflammation and organ damage associated with deletion of HMGB1 was ameliorated by PARP-1 inhibition

Our above findings demonstrate that PARP-1 over-activation in cells lacking HMGB1 may lead to cellular damage. Interestingly, inhibition of PARP-1 has been shown to protect the liver and heart from I/R induced injury (22). To determine if the increased hepatocyte damage from loss of HMGB1 could be prevented with PARP-1 inhibition, we treated hypoxic hepatocytes from either HMGB1-HC-KO or control mice with the PARP-1 inhibitors PJ-34 or 3-AB. The supernatants from these hepatocytes were added to hepatic NPCs and the production of TNF-α, IL-6 and IL-1β were measured. The PARP-1 inhibitors treatment in hypoxic hepatocytes blocked the cytokine production from hypoxic media-treated NPC (Fig.7C and Supplemental Fig.5C). To further confirm the role of PARP-1 in contributing to the enhanced injury in mice lacking HMGB1, we also treated mice with PARP-1 inhibitors during liver I/R. PJ-34 or 3-AB significantly reduced hepatic injury in both HMGB1-HC-KO and control mice following I/R, however the effect was more pronounced in the HMGB1-HC-KO mice (Fig.7D and Supplemental Fig.5D). These results further solidify the importance of PARP-1 in the injurious oxidative stress response of HMGB1 deficient hepatocytes.

DISCUSSION

This study was undertaken to elucidate the cell specific roles of HMGB1 in the setting of liver I/R injury. Previously, the consequences of the lack of HMGB1 have been difficult to define secondary to mice deficient in HMGB1 dying shortly after birth (9). Therefore, we have developed conditional KO mice to investigate the roles of HMGB1 within hepatocytes. We had postulated that hepatocyte HMGB1 deletion would reduce liver damage during I/R because of the known role for extracellular HMGB1 in driving inflammation-associated injury in I/R (25). Instead, we found that HMGB1-HC-KO mice are much more sensitive to damage in liver I/R revealing dominant intracellular roles of HMGB1 during redox stress. In this study we have illustrated that the lack of HMGB1 leads to several detrimental cellular changes during oxidative stress including: 1) Increased DNA damage and decreased chromatin accessibility to repair; 2) Excessive nuclear instability and release of nucleosome components leading to activation of the PRR, TLR9; and 3) Activation of PARP-1 is increased, leading to decreased energy stores, with subsequent mitochondrial injury and ROS production.

The generation of ROS after I/R is one of the primary early events with many cellular consequences including membrane lipid peroxidation, oxidative changes in protein structure/function, and oxidative damage to DNA (22). DNA bases are prone to oxidation leading to detrimental effects in replication and transcription if not repaired via either NER or BER depending on lesion (18). In addition to many other roles, HMGB1 also plays critical roles in NER and BER (8). Previous work with mouse embryonic fibroblasts found that cells lacking HGMB1 are hypersensitive to DNA damage by UV irradiation, leading to increased mutagenesis, chromosomal instability, and decreased cell survival (26, 27). Normally, acetylation of histones H3 and H4 is increased after DNA damage, allowing for chromatin accessibility and subsequent repair (28). However, we found that within HMGB1-HC-KO mice there was decreased acetylation of histones H3 and H4, suggesting that HMGB1 in hepatocytes is essential for providing chromatin accessibility induced by DNA damage after liver I/R injury. Similar to our finding, Lange et al. have previously shown that mouse embryonic fibroblasts lacking HMGB1 have decreased histone acetylation after UVC irradiation (27). Increased DNA damage in HMGB1-HC-KO mice was further confirmed with increased phosphorylation of γ-H2AX, a marker of DNA damage.

Oxidative damage to DNA subsequently leads to the activation of several nuclear repair enzymes such as PARP-1. Ordinarily, with low levels of DNA damage, PARP-1 alters chromatin structure and facilitates DNA repair (29). However, with excessive DNA damage PARP-1 may lead to cell death (30). PARP-1, activated by DNA damage, uses NAD^+ as a substrate for PAR formation on target proteins, facilitating nuclear DNA repair (21). However, excessive DNA damage leads to over-activation of PARP-1, which may lead to NAD^+ depletion, exhausting ATP stores (21, 22). NAD^+ depletion may subsequently lead to the failure of NAD^+-dependent processes, in addition to the opening of mitochondrial permeability transition pores (MPT), uncoupling of oxidative phosphorylation, and mitochondrial failure (31). PARP-1 inhibition or PARP-1 deficiency has been demonstrated to prevent organ damage from liver I/R injury (32-34). Additionally, there is evidence that PARP-1 activation inhibits the recovery of damaged mitochondria (22). Sustained

mitochondrial depolarization leads to further oxidant stress, perpetuating cellular injury. Indeed, in this study we have found that with lack of HMGB1 there is increased PARP-1 activation and reduced NAD^+, which leads to increased mitochondrial injury and subsequently increases both total cellular and mitochondrial ROS generation. Thus providing one mechanism for the increased hepatocellular injury seen within the HMGB1-HC-KO mice after hepatic I/R.

Downstream from cellular injury there is release of nucleosome components, including DNA and histones, which may then activate the TLR9 signaling pathway, propagating the sterile inflammatory response. We have previously demonstrated that the protective effects of blocking extracellular histones and the detrimental effects of exogenous histones in hepatic I/R are dependent on TLR9 signaling (14). In this study we have further supported that the activation of TLR9 signaling exacerbates the injury associated with lack of hepatocyte HMGB1. Inhibition of TLR9 did indeed abrogate the increased injury seen in HMGB1-HC-KO mice subjected to hepatic I/R.

In summary, we use novel hepatocyte-specific transgenic HMGB1 KO mice to investigate the role of HMGB1 within hepatocytes subjected to oxidative stress, either via I/R or hypoxia exposure. The increased injury and inflammatory response seen in these HMGB1-HC-KO mice is in part related to increased DNA damage and nuclear instability with resultant increased release of histones. Diagrammatic summarization of the key findings of this study is shown **(**Fig.8**)**. Interestingly, we have found that HMGB1 may serve dichotomous roles after a sterile inflammatory insult, having both a beneficial intracellular role and injurious extracellular role. The novel findings of this study help to dissect out the essential role of HMGB1 during cellular stress, suggesting that the intracellular role of HMGB1 during sterile inflammatory response may even outweigh its function as an extracellular signaling molecule and DAMP.

Supplementary Material

Refer to Web version on PubMed Central for supplementary material.

Acknowledgments

We thank Xinghuang Liao, Nicole Hays and Junda Chen for technical assistance in preparing the manuscript.

Financial Support: This work was supported by Howard Hughes Medical Institute Physician-Scientist Award (A.T.), Association of Academic Surgery Foundation Research Fellowship Award (G.N.), R01-GM95566 (A.T.), R01-GM50441 (T.B.).

List of Abbreviations

DAMP	Damage associated molecular pattern
PAMP	Pathogen associated molecular pattern
PRR	pattern recognition receptor
TLR	Toll-Like Receptor

I/R	Ischemia/Reperfusion
HMGB1	High Mobility Group Box 1

REFERENCES

1. Fondevila C, Busuttil RW, Kupiec-Weglinski JW. Hepatic ischemia/reperfusion injury--a fresh look. Experimental and Molecular Pathology. 2003; 74:86–93. [PubMed: 12710939]
2. Huang H, Evankovich J, Yan W, Nace G, Zhang L, Ross M, Liao X, et al. Endogenous histones function as alarmins in sterile inflammatory liver injury through toll-like receptor 9. Hepatology. 2011
3. Tsung A, Klune JR, Zhang X, Jeyabalan G, Cao Z, Peng X, Stolz DB, et al. HMGB1 release induced by liver ischemia involves Toll-like receptor 4 dependent reactive oxygen species production and calcium-mediated signaling. J Exp Med. 2007; 204:2913–2923. [PubMed: 17984303]
4. Tsung A, Sahai R, Tanaka H, Nakao A, Fink MP, Lotze MT, Yang H, et al. The nuclear factor HMGB1 mediates hepatic injury after murine liver ischemia-reperfusion. The Journal of experimental medicine. 2005; 201:1135–1143. [PubMed: 15795240]
5. Javaherian K, Liu JF, Wang JC. Nonhistone proteins HMG1 and HMG2 change the DNA helical structure. Science. 1978; 199:1345–1346. [PubMed: 628842]
6. Tang D, Kang R, Livesey KM, Zeh HJ III, Lotze MT. High mobility group box 1 (HMGB1) activates an autophagic response to oxidative stress. Antioxid.Redox.Signal. 2011; 15:2185–2195. [PubMed: 21395369]
7. Klune JR, Dhupar R, Cardinal J, Billiar TR, Tsung A. HMGB1: endogenous danger signaling. Molecular medicine. 2008; 14:476–484. [PubMed: 18431461]
8. Lange SS, Vasquez KM. HMGB1: the jack-of-all-trades protein is a master DNA repair mechanic. Molecular carcinogenesis. 2009; 48:571–580. [PubMed: 19360789]
9. Calogero S, Grassi F, Aguzzi A, Voigtlander T, Ferrier P, Ferrari S, Bianchi ME. The lack of chromosomal protein Hmg1 does not disrupt cell growth but causes lethal hypoglycaemia in newborn mice. Nat Genet. 1999; 22:276–280. [PubMed: 10391216]
10. Nace GW, Huang H, Klune JR, Eid RE, Rosborough BR, Korff S, Li S, et al. Cellular specific role of toll-like receptor 4 in hepatic ischemia-reperfusion injury. Hepatology. 2013
11. Tsung A, Hoffman RA, Izuishi K, Critchlow ND, Nakao A, Chan MH, Lotze MT, et al. Hepatic ischemia/reperfusion injury involves functional TLR4 signaling in nonparenchymal cells. J Immunol. 2005; 175:7661–7668. [PubMed: 16301676]
12. Huang H, Deng M, Jin H, Liu A, Dirsch O, Dahmen U. Hepatic arterial perfusion is essential for the spontaneous recovery from focal hepatic venous outflow obstruction in rats. American journal of transplantation : official journal of the American Society of Transplantation and the American Society of Transplant Surgeons. 2011; 11:2342–2352.
13. Sun Q, Gao W, Loughran P, Shapiro R, Fan J, Billiar TR, Scott MJ. Caspase-1 activation is protective against hepatocyte cell death by up-regulating beclin1 and mitochondrial autophagy in the setting of redox stress. J Biol Chem. 2013
14. Huang H, Evankovich J, Yan W, Nace G, Zhang L, Ross M, Liao X, et al. Endogenous histones function as alarmins in sterile inflammatory liver injury through Toll-like receptor 9 in mice. Hepatology. 2011; 54:999–1008. [PubMed: 21721026]
15. Loughran PA, Stolz DB, Barrick SR, Wheeler DS, Friedman PA, Rachubinski RA, Watkins SC, et al. PEX7 and EBP50 target iNOS to the peroxisome in hepatocytes. Nitric oxide : biology and chemistry / official journal of the Nitric Oxide Society. 2013; 31:9–19. [PubMed: 23474170]
16. Stolz DB, Ross MA, Salem HM, Mars WM, Michalopoulos GK, Enomoto K. Cationic colloidal silica membrane perturbation as a means of examining changes at the sinusoidal surface during liver regeneration. The American journal of pathology. 1999; 155:1487–1498. [PubMed: 10550305]

17. Bamboat ZM, Ocuin LM, Balachandran VP, Obaid H, Plitas G, DeMatteo RP. Conventional DCs reduce liver ischemia/reperfusion injury in mice via IL-10 secretion. J Clin Invest. 2010; 120:559–569. [PubMed: 20093775]
18. Cooke MS, Evans MD, Dizdaroglu M, Lunec J. Oxidative DNA damage: mechanisms, mutation, and disease. The FASEB journal : official publication of the Federation of American Societies for Experimental Biology. 2003; 17:1195–1214.
19. Zentner GE, Henikoff S. Regulation of nucleosome dynamics by histone modifications. Nat Struct Mol Biol. 2013; 20:259–266. [PubMed: 23463310]
20. Gibson BA, Kraus WL. New insights into the molecular and cellular functions of poly(ADP-ribose) and PARPs. Nat Rev Mol Cell Biol. 2012; 13:411–424. [PubMed: 22713970]
21. Rouleau M, Patel A, Hendzel MJ, Kaufmann SH, Poirier GG. PARP inhibition: PARP1 and beyond. Nat Rev Cancer. 2010; 10:293–301. [PubMed: 20200537]
22. Schriewer JM, Peek CB, Bass J, Schumacker PT. ROS-mediated PARP activity undermines mitochondrial function after permeability transition pore opening during myocardial ischemia-reperfusion. J Am Heart Assoc. 2013; 2:e000159. [PubMed: 23598272]
23. Ryter SW, Kim HP, Hoetzel A, Park JW, Nakahira K, Wang X, Choi AM. Mechanisms of cell death in oxidative stress. Antioxid Redox Signal. 2007; 9:49–89. [PubMed: 17115887]
24. Esterbauer H, Schaur RJ, Zollner H. Chemistry and biochemistry of 4-hydroxynonenal, malonaldehyde and related aldehydes. Free Radic Biol Med. 1991; 11:81–128. [PubMed: 1937131]
25. Tsung A, Hoffman RA, Izuishi K, Critchlow ND, Nakao A, Chan MH, Lotze MT, et al. Hepatic ischemia/reperfusion injury involves functional TLR4 signaling in nonparenchymal cells. J.Immunol. 2005; 175:7661–7668. [PubMed: 16301676]
26. Giavara S, Kosmidou E, Hande MP, Bianchi ME, Morgan A, d'Adda di Fagagna F, Jackson SP. Yeast Nhp6A/B and mammalian Hmgb1 facilitate the maintenance of genome stability. Current biology : CB. 2005; 15:68–72. [PubMed: 15649368]
27. Lange SS, Mitchell DL, Vasquez KM. High mobility group protein B1 enhances DNA repair and chromatin modification after DNA damage. Proceedings of the National Academy of Sciences of the United States of America. 2008; 105:10320–10325. [PubMed: 18650382]
28. Ramanathan B, Smerdon MJ. Changes in nuclear protein acetylation in u.v.-damaged human cells. Carcinogenesis. 1986; 7:1087–1094. [PubMed: 3087643]
29. Peralta-Leal A, Rodriguez-Vargas JM, Aguilar-Quesada R, Rodriguez MI, Linares JL, de Almodovar MR, Oliver FJ. PARP inhibitors: new partners in the therapy of cancer and inflammatory diseases. Free Radic Biol Med. 2009; 47:13–26. [PubMed: 19362586]
30. Szabo C, Dawson VL. Role of poly(ADP-ribose) synthetase in inflammation and ischaemia-reperfusion. Trends Pharmacol Sci. 1998; 19:287–298. [PubMed: 9703762]
31. Tao R, Kim SH, Honbo N, Karliner JS, Alano CC. Minocycline protects cardiac myocytes against simulated ischemia-reperfusion injury by inhibiting poly(ADP-ribose) polymerase-1. Journal of cardiovascular pharmacology. 2010; 56:659–668. [PubMed: 20881608]
32. Khandoga A, Enders G, Biberthaler P, Krombach F. Poly(ADP-ribose) polymerase triggers the microvascular mechanisms of hepatic ischemia-reperfusion injury. Am J Physiol Gastrointest Liver Physiol. 2002; 283:G553–560. [PubMed: 12181167]
33. Szijarto A, Batmunkh E, Hahn O, Mihaly Z, Kreiss A, Kiss A, Lotz G, et al. Effect of PJ-34 PARP-inhibitor on rat liver microcirculation and antioxidant status. The Journal of surgical research. 2007; 142:72–80. [PubMed: 17612561]
34. Mota-Filipe H, Sepodes B, McDonald MC, Cuzzocrea S, Pinto R, Thiemermann C. The novel PARP inhibitor 5-aminoisoquinolinone reduces the liver injury caused by ischemia and reperfusion in the rat. Medical science monitor : international medical journal of experimental and clinical research. 2002; 8:BR444–453. [PubMed: 12444369]

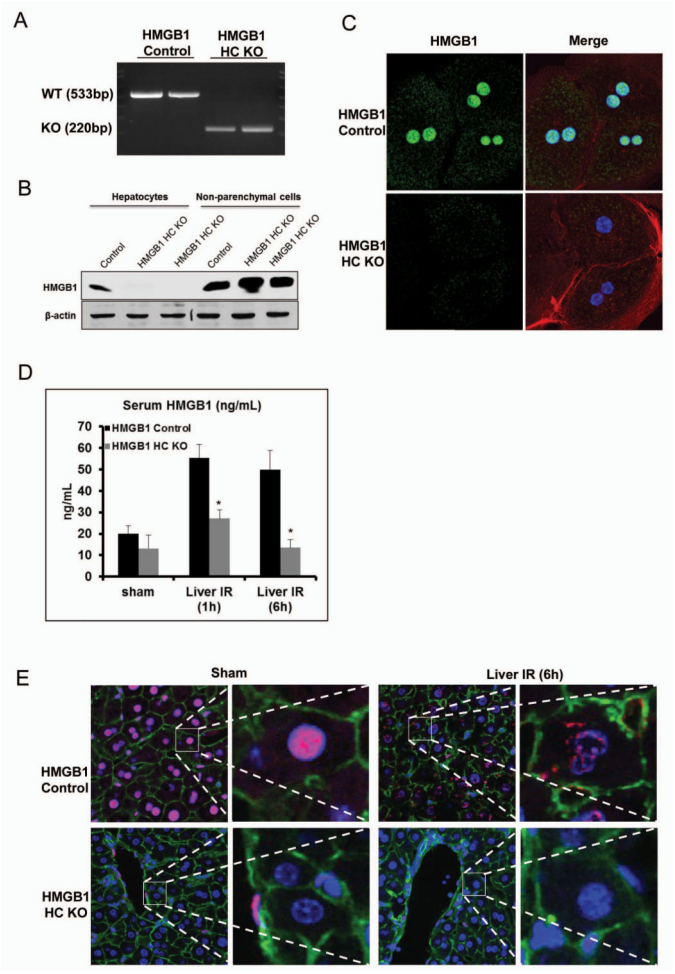

Figure 1. Confirmation of specificity of HMGB1 knockout (HMGB1-HC-KO)

(A) RT-PCR was used to determine mRNA levels of HMGB1 within isolated hepatocytes from control and HMGB1-HC-KO mice. (B) HMGB1 protein levels within isolated hepatocytes or non-parenchymal cells from control and HMGB1-HC-KO mice were assessed by Western blot analysis. Figure is representative of three experiments with similar results. (C) Immunofluorescent stain of HMGB1 within cultured hepatocytes from control and HMGB1-HC-KO mice (magnification ×400). Images are representative of three experiments with similar results. Green, HMGB1; blue, nuclei; red, F-actin. (D) Serum HMGB1 ELISA after 1h or 6h of reperfusion. *P<0.05 when compared against control. (E) Immunofluorescent stain of HMGB1 within from sections of normal liver and liver 6h after I/R in control and HMGB1-HC-KO mice (magnification ×400). Images are representative liver sections from six mice per group. Red, HMGB1; blue, nuclei; green, F-actin.

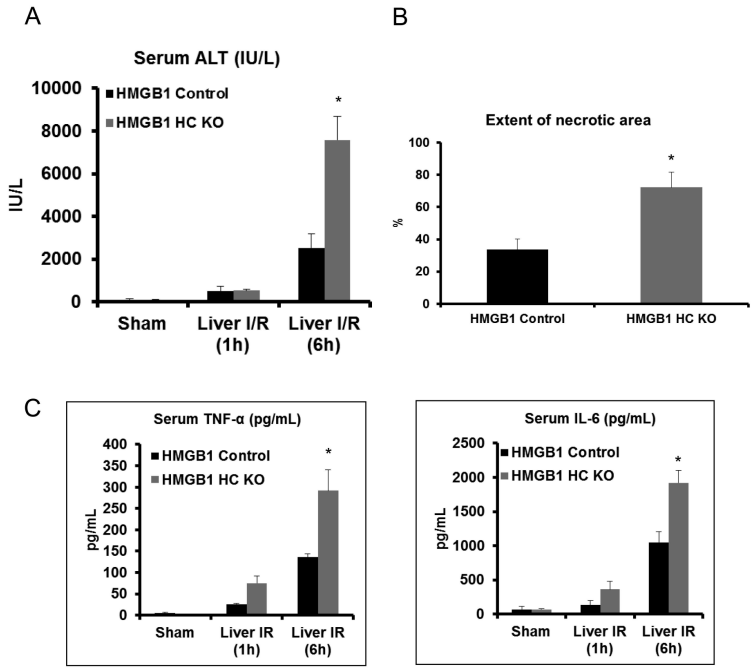

Figure 2. Cellular specific role of HMGB1 on hepatocellular injury after I/R

(A) Serum ALT levels were analyzed in control and HMGB1-HC-KO mice after either sham laparotomy or 1h of ischemia and 1h or 6h of reperfusion. Data represent the mean ± SE (n = 6 mice per group). *P < 0.05 vs. HMGB1 control. (B) Quantification of necrotic hepatocytes in H&E-stained liver sections (Supplemental Figure 2B) from HMGB1-HC-KO and control mice 6h after reperfusion. The graph is representative of liver sections from six mice per group. *P < 0.05 vs. control. (C) Serum levels of TNF-α and IL-6 obtained from HMGB1-HC-KO and control mice at 6h after reperfusion were measured by ELISA and compared to the sham group. Data represent the mean ± SE (n = 6 mice per group) *P<0.05 vs. control.

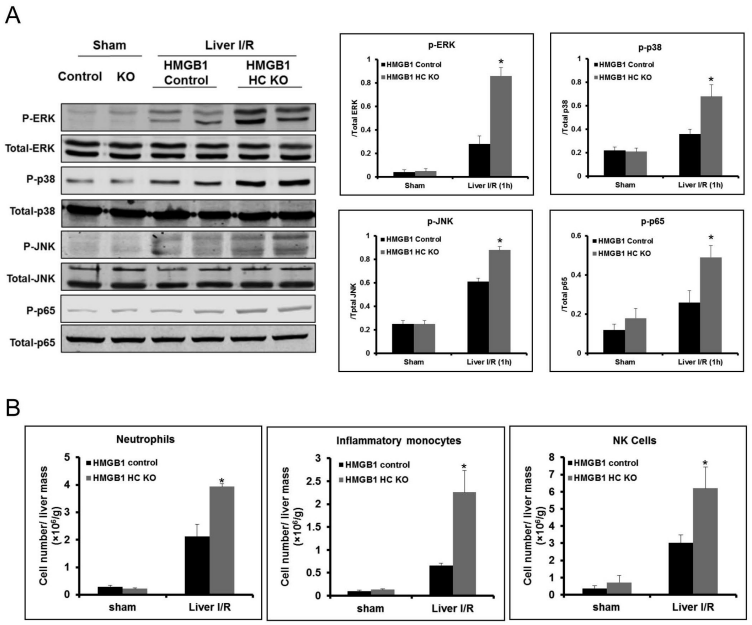

Figure 3. Lack of HMGB1 in hepatocytes mediates inflammatory signaling and regulates innate immune cells in liver I/R

(A) Mitogen-activated protein kinase activation and phosphorylation at serine 536 of the p65 subunit of NF-κB were determined by Western blot and quantitative densitometry analysis of the protein expressions in sham-treated mice and mice that underwent ischemia and 1h of reperfusion. Hepatic protein lysates from ischemic lobes were obtained; each lane represents a separate animal. The blots shown are representative of three experiments with similar results. *P < 0.05 vs. control. (B) Flow cytometry analysis with a quantitative evaluation of NPCs in homogenized ischemia liver lobes in HMGB1-HC-KO and control mice. Fold change of cell numbers of neutrophils, inflammatory monocytes cells, and nature killer (NK) cells. Data represent the mean ± SE (n = 6 mice per group). *P < 0.05 compared to sham mice. Each experiment was repeated a minimum of three times.

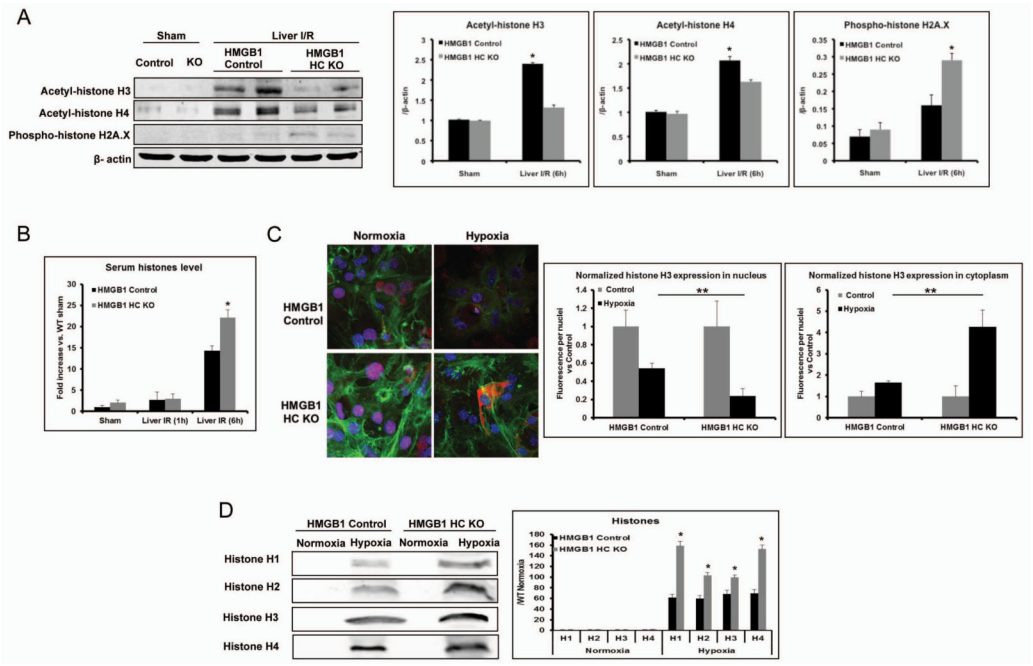

Figure 4. Lack of HMGB1 in hepatocytes leads to less DNA repair and more DNA damage, with subsequently more cell death and histone release

(A) Acetylation of histone H3 and H4, and phosphorylation of H2A.X were determined by Western blot and quantitative densitometry analysis in sham-treated mice and mice that underwent ischemia and 6h of reperfusion. Hepatic protein lysates from ischemic lobes were obtained; each lane represents a separate animal. The blots shown are representative of three experiments with similar results. *P < 0.05 vs. control. (B) Serum histone levels were assessed after I/R using ELISA. Data represent the mean ± SE (n = 6 mice per group). *P < 0.05 compared to control. (C) The translocation of histone H3 in cultured hepatocytes from HMGB1-HC-KO or control mice that were stimulated with either hypoxia or normoxic for 12h was visualized and observed under confocal microscope (magnification ×400). Green, actin; blue, nuclei; red, histone H3. Quantitation of nucleic or cytoplasmic histone H3 in cultured hepatocytes from HMGB1-HC-KO or control mice was measured using the analytical software MetaMorph™ and normalized to nuclei within the sample field. *P < 0.05; hypoxia vs. normoxia control, **P < 0.05; HMGB1-HC-KO vs. control. (D) Cultured hepatocytes from HMGB1-HC-KO or control mice were exposed to hypoxia. Media were subjected to Western blot and quantitative densitometry analysis of histone H1, H2, H3, and H4. The blots shown are representative of three experiments with similar results. *P < 0.05 vs. control.

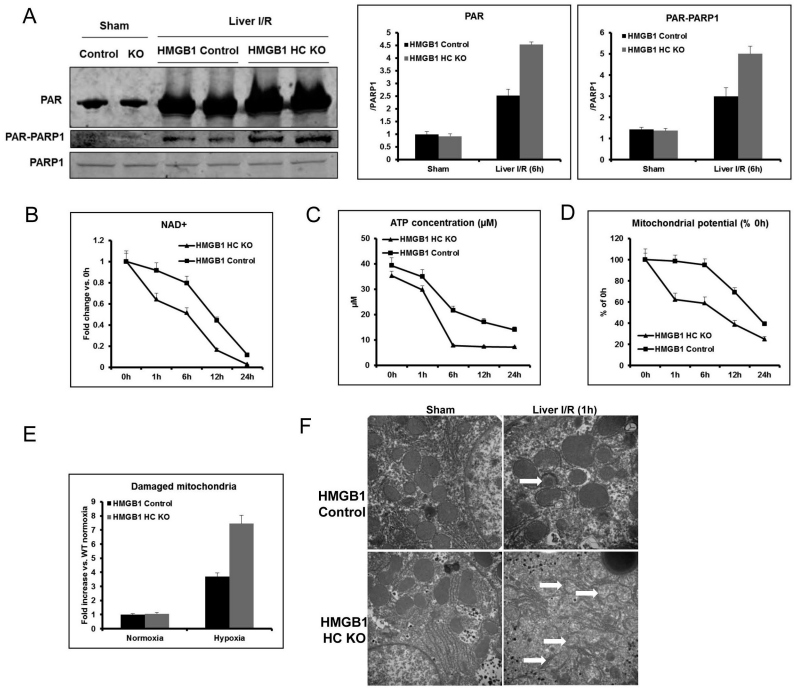

Figure 5. Lack of HMGB1 in hepatocytes induces PARP-1 over-activation, damages mitochondria by exhausting NAD^+ and ATP

(A) Total PAR formation and Poly (ADP-ribosylation) of PARP-1 was determined by Western blot and quantitative densitometry analysis of the protein expressions in sham-treated mice and mice that underwent ischemia and 6h of reperfusion. Hepatic protein lysates from ischemic lobes were obtained; each lane represents a separate animal. The blots shown are representative of three experiments with similar results. *P < 0.05 vs. control. (B) Time course of NAD^+ level in cultured hepatocytes from HMGB1-HC-KO or control mice during hypoxia (n=4-6 for each point). *P < 0.05 vs. control. (C) Time course of ATP level in cultured hepatocytes from HMGB1-HC-KO or control mice during hypoxia (n=4-6 for each point). *P < 0.05 vs. control. (D) Time course of mitochondrial potential in cultured hepatocytes from HMGB1-HC-KO or control mice during hypoxia (n=4-6 for each point). *P < 0.05 vs. control. (E) HMGB1 KO or control hepatocytes were cultures under normoxia or 12h hypoxia. The cells were then stained with 200nM MitoTracker Green and MitoTracker Deep Red (Invitrogen) for 45min at 37°C then analyzed using flow cytometry for mitochondrial damage. *P < 0.05 vs. control. (F) Mitochondrial ultrastructure from livers of HMGB1-HC-KO or control mice following sham or 1h reperfusion were imaged by transmission electron microscope (magnification ×50000). *, P<0.05; results are representative of 3 separate independent experiments. White arrows point to damaged mitochondrial cristae.

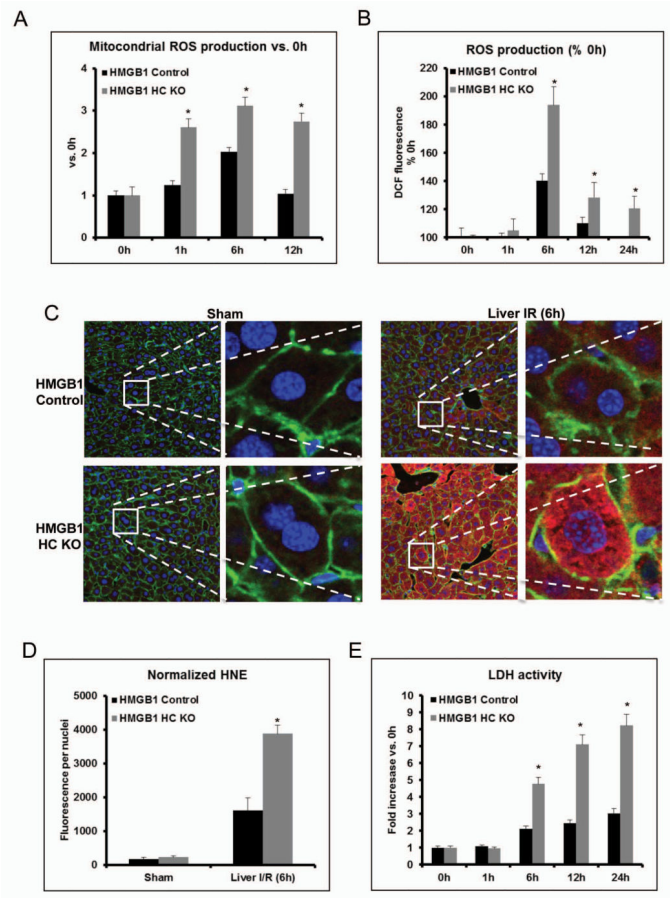

Figure 6. Lack of HMGB1 in hepatocytes mediates mitochondrial and cellular ROS production

(A) Flow cytometry of cultured hepatocytes from HMGB1-HC-KO or control mice that were stimulated with hypoxia and stained with MitoSOX to determine mitochondrial ROS production. The bar graph represents pooled data from three experiments. 0h represents normoxia. *P < 0.05 compared to PBS treatment. (B) Cellular ROS production as detected by the DCF-DA assay in cultured whole hepatocytes, which were obtained from either HMGB1-HC-KO or HMGB1 control mice. 0h represents normoxia. *P < 0.05 compared to control. (C) Representative 4-HNE staining Green, actin; blue, nuclei; 4-HNE, red and (D) quantification of 4-hydroxy-2-nonenal (4-HNE) adducts (4-HNE normalized per nuclei in the field) in ischemic liver of HMGB1-HC-KO or control mice. *P < 0.05 compared to control. (E) Time course of LDH activity in cultured hepatocytes from HMGB1-HC-KO or control mice during hypoxia (n=4-6 for each point). *P < 0.05 vs. control.

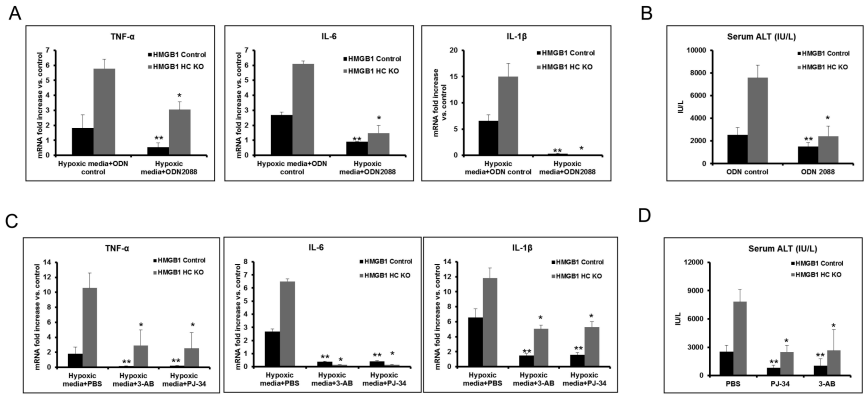

Figure 7. Addition of TLR9 antagonists and PARP-1 inhibitors both protect HMGB1-HC-KO mice from liver I/R injury

(A) TNF-α, IL-6 and IL-1β mRNA expression was determined in non-parenchymal cells cultured overnight with media from hypoxic HMGB1 KO or control hepatocytes. Non-parenchymal cells were treated with TLR9 antagonist, ODN2088, or ODN control. Results are expressed as the relative increase of mRNA expression compared with PBS treatment. Data represent the mean ± SE and are representative of three experiments with similar results. *P < 0.05 compared to ODN control-treated HMGB1-HC-KO group. **P < 0.05 compared to ODN control-treated HMGB1 Control group. (B) Serum ALT levels in HMGB1-HC-KO or control mice after 6h of reperfusion that were treated with ODN2088 or ODN control. Data represent the mean ± SE (n = 6 mice per group). *P < 0.05 compared to ODN control-treated HMGB1-HC-KO group. **P < 0.05 compared to ODN control-treated HMGB1 Control group. (C) TNF-α, IL-6 and IL-1β mRNA expression was determined in non-parenchymal cells cultured overnight with media from hypoxic HMGB1 KO or control hepatocytes. Hepatocytes were pre-treated with the PARP-1 inhibitor, 3-AB or PJ-34, or negative control, PBS. Results are expressed as the relative increase of mRNA expression compared with PBS treatment. Data represent the mean ± SE and are representative of three experiments with similar results. *P < 0.05 compared to PBS-treated HMGB1-HC-KO group. **P < 0.05 compared to PBS-treated HMGB1 Control group. (D) Serum ALT levels in HMGB1-HC-KO or control mice after 6h of reperfusion that were treated with the PARP-1 inhibitor, 3-AB or PJ-34, or PBS. Data represent the mean ± SE (n = 6 mice per group). *P < 0.05 compared to PBS-treated HMGB1-HC-KO group. **P < 0.05 compared to PBS-treated HMGB1 Control group.

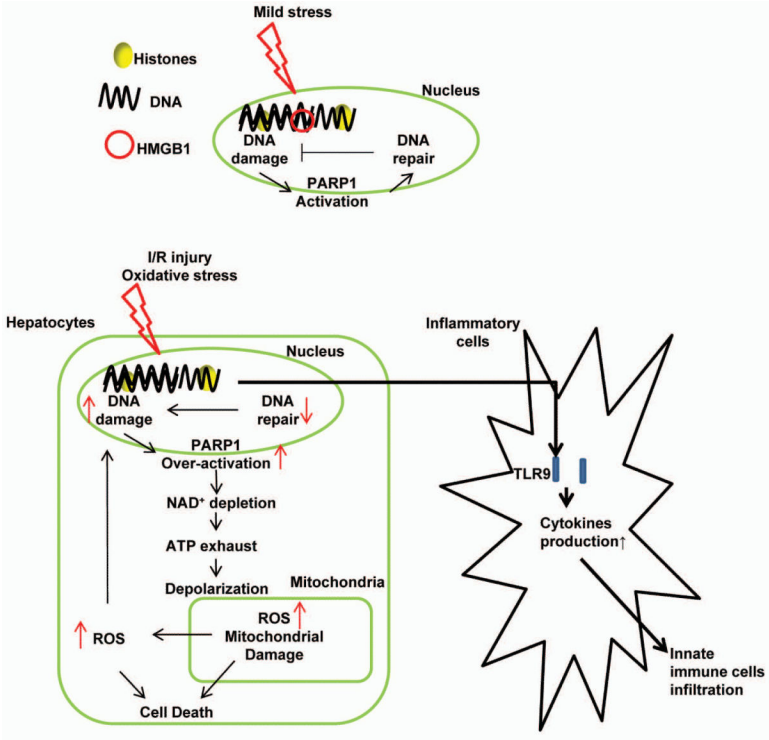

Figure 8.

Schematic representation of the intracellular role of HMGB1 during liver I/R injury. During liver I/R injury, HMGB1 deletion in hepatocytes leads to excessive DNA damage, which initiates over-activation of PARP-1, subsequently exhausting both NAD+ and ATP reserves, damaging mitochondria by depolarization of the mitochondrial membrane. Damaged mitochondria are associated with more mitochondrial and cellular ROS production, eventually leading to more cell stress and death. Excessive cell death further propagates the inflammatory response and infiltration of innate immune cells in liver I/R by released histones.